

Thermal behavior of natural convection flow in an inclined solar air heater

Mohammed A. Neama and Ayad T. Mustafa*

Mechanical Engineering Department, College of Engineering, Al-Nahrain University, Jadiriya, Baghdad, Iraq
Phone: +9647736259862

ABSTRACT – The thermal behavior of hot air in a natural convection mode on a solar absorber-plate has not been, so far, modeled experimentally. The present work aimed to assess the performance of the inclined solar air heater [SAH] experimentally by investigating the temperature distribution field in the natural convection flow. The solar plate collector is designed based on the aspect ratio of length to height, L / H , of 6 and 12. The measurements are carried out for the collector tilt angles of 30°, 45°, 60° and 75°. The present investigation demonstrates the temperature distribution of hot air floated in an inclined channel of the SAH. The investigation showed 2D thermal stratification increases when increasing the distance along the collector plate, which looks clear in the SAH with a height of 10 cm. The results of the study show that the thickness of the thermal layers increases with increasing the tilt angle from 30° to 75°. The reason dates back to increasing the buoyancy force of the hot air over the absorber. The results demonstrated that the air temperatures for the height of 0.1 m and 45° tilt angle are higher than that for the height of 0.2 m by 23%.

ARTICLE HISTORY

Received: 16th Mar 2020

Revised: 18th July 2020

Accepted: 17th Aug 2020

KEYWORDS

Solar air heater;
thermal behavior;
temperature stratification;
solar irradiance;
inclination angle;
collector height

INTRODUCTION

The solar collectors are receivers of solar irradiance, which are utilized to transform the solar irradiance into the heat energy by raising the temperature of the fluid streaming within the collector. The solar irradiance is received either by non-concentrated collector or concentrated collector. The non-concentrated solar plate collectors can be classified into a water heater and air heater, SAH.

The main parts of the solar air heater are; first, absorber-plate made from metal (copper, aluminum, or steel), where the plate could be coated by black material with high absorptivity (α). Second, translucent cover that allows the irradiance to transmit through in with properties of high transmission (τ), low reflection (ρ) and absorption (α), such as glass or Perspex. Third, the thermal insulation material used to keep generated heat in an absorber plate [1].

The air heating process is relying on the irradiance absorbed by the plate. The absorbed energy is then converted into heat which appears as temperature rise in the plate. Due to the convection heat transfer, air temperatures over the heated absorber plate will increase [2]. SAH are utilized in different implementations such as; space heating, electricity production, air-conditioning, and fruits drying [3].

For an internal airflow over a heated plate in a short channel (small length to height), the thermal layer are producing over the plate. The buoyancy force component becomes an active parameter in the normal and parallel direction to the streamlines specially in an inclined channel [4, 5]. Thermal analysis of the SAH shown in Figure 1, as a short channel, is relying on the convection heat transfer in natural mode between the absorber and the airflow.

The convection heat transfer in natural mode over a heated plate in a short channel has investigated. Thermal-flow variation has tested by determining the non-dimensional terms named Nusselt number, Grashof number, and Prandtl numbers. Hollands et al. [6] offered an experimental study of convection flow in natural mode between two inclined layers heated from the bottom with a high aspect ratio. Experimental tests have covered by the range of the Rayleigh number from 105 to 1708 and inclination angle from 0° to 70°. A relationship between the Rayleigh number with the Nusselt number was determined. Beikircher et al. [7] investigated the free convection that occurs inversely between two plates in parallel situation separated by a distance ranged from 2cm to 10cm, which the upper plate heated electrically. The experiments have carried out in an inclination angle ranged from 0° to 90°. Temperature variation on the heated plate was recorded whereas the down plate kept cold. It was found the mean plate temperatures that adapted to 90°C and 30°C are producing with Rayleigh numbers between 2.7×10^4 and 3.3×10^6 , respectively. Siddiqua et al. [8] studied numerically the thermal layer of natural convection flowing on an inclined plate heated internally. Results show that heat generation, inclination angle, and viscosity have a significant effect on the temperature and velocity distributions.

Due to solar irradiance received by flat-plate facing south, a natural convection flow has generated on the upper side and investigated experimentally and theoretically. Two modes of convection heat transfer, natural and forced, were tested by determining the coefficient of convection heat transfer between the plate and the airflow in the non-dimensional term named Nusselt number. Hernández et al. [9] offered an analytical model that validated experimentally for the performance of natural convection flow in the double side's air heater. The results have revealed the useful heat

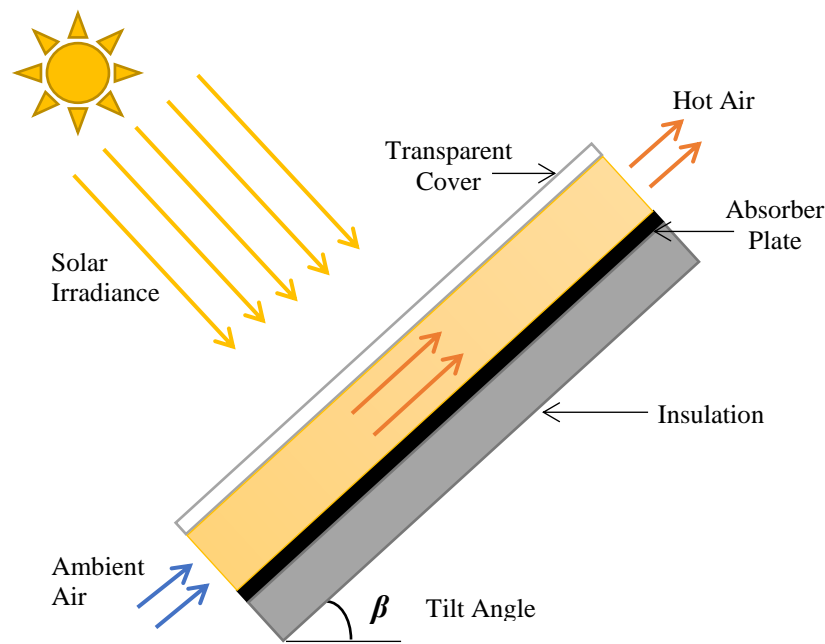


Figure 1. Schematic of inclined solar air heater

obtained and output temperature, where the efficiency of the solar air collector ranged from 0.48 to 0.5 on sunny days. Hematian and Bakhtiari [10] studied experimentally the heat transfer in two convection modes inside the air heater with the thermal efficiency evaluation. It was concluded that the efficiency in forced mode is lower than in natural mode, whereas low air temperature decreases the heat loss from the collector. Bagga [11] modeled numerically and experimentally the solar air collector with two convection modes of heat transfer. The solar collector has a double glass covering. Results show increasing the heat transfer to air when the number of passages in the solar collector increases. Bahrehmand and Ameri [12] modeled mathematically a single and double glazing air heater with natural convection heat transfer. Mathematical modeling was based on energy balance for the collector parameters. Predicted results showed that the solar collector with double glazing has better thermal performance than a single glass. Demou and Grigoriadis [13] presented a seasonal energy model of the air heater, which utilizes the meteorological data, geometrical materials, and solar orientation. This model was built to predict temperatures, heat transfer, efficiency, absorber-cover spacing, absorber material, and orientation. Kumar and Premachandran [14] investigated numerically the heat transfer in natural convection mode within the solar collector via simulated as a 3D rectangular channel in an inclined position. The input parameters of ambient wind velocity, heat flux, and tilt angle are varied between 0.0-1.0 m/s, 250-750 W/m², and 15°- 60°, respectively. Results reveal that when wind velocity is zero, the flow inside the heater is powered by buoyancy force only. Whilst, mixed convection produces in the heater channel in the presence of the ambient wind, therefore heat transfer from the plate increases and outlet air temperature decreases. Also, the convection heat transfer rises within the heater channel when inclined up to 45° and zero wind velocity. Mzad et al. [15] evaluated experimentally an influence of the tilt angle of the solar collector on the thermal efficiency. To receive the maximum irradiance, the solar air collector inclination has been changed between 15° to 70°. The results show that the maximum useful power is obtained for an inclination angle varied between 15° and 30°, while it decreases for tilt angle up to 45° due to decrease in received irradiance.

The performance of solar air collectors has investigated by improving thermal efficiency. The improvements have been carried out experimentally and theoretically by increasing the heat transfer to airflow or decreasing the heat loss to surroundings. The thermal efficiency of the improved solar air collector is increasing in comparison with traditional air heater by raising the convection heat transfer by integrating different shapes into the solar collector, such as bells [16], barriers [17], small tubes [18, 19], and tubular air heater in dual passage [20]; or by using porous plate [21].

Based on the previous literature survey, natural convection heat transfer and the thermal layer produced over a flat-plate heated electrically have investigated theoretically and experimentally by using the non-dimensional terms. On the other hand, performance improvement and convection heat flow produced over the absorber plate within the air heater was investigated theoretically and experimentally by determining, frequently, the heat transfer coefficient in natural convection mode between the plate and the airflow.

Nevertheless, the thermal behavior in the bare SAH channel (i.e. no external shapes over the plate) as temperature distribution over the solar absorber-plate has not been, so far, modeled and analyzed experimentally. Hence, the present work aimed to assess the SAH performance experimentally by investigating the 2D temperature distribution field in the natural convection flow. Also, study the effect of collector tilt angle, collector height, and solar irradiance on the SAH efficiency.

RESEARCH METHODOLOGY

Design of Test Section

The temperature rise in the solar air collector is relying on the solar irradiance, area of the collector, and materials of absorber and canopy. The solar air heater model in the present work is utilized in heating air by free convection, where materials of the absorber-plate and the cover would be black painted galvanized steel and glass, respectively. The received total irradiance (direct and diffuse) is heating the absorber and produces a hot airflow in one dimension within the collector from the inlet to the outlet by a buoyant force effect. Therefore, dimensions of the designed model based on the collector length, L , and height, H , where an aspect ratio of length to height, L/H , is a significant parameter.

For the present experimental model, an aspect ratio described in Table 1 is utilized in the designing, where L/H of 6 and 12 have chosen. The collector length is assumed to be 1.2 m, then for aspect ratio of 6, the collector height will be 0.2 m, and for aspect ratio of 12, the collector height will be 0.1 m.

Table 1. The collector aspect ratio to the critical angle [5]

L/H	1	3	6	12	>12
β_{cr}	25°	53°	60°	67°	70°

The solar air collector designed according to Çengel and Ghajar conditions [5]. Hence, the Nusselt number for inclined SAH can be estimated for $0 < \beta < \beta_{cr}$ and $L/H < 12$ by:

$$Nu_{\beta} = Nu_{\beta=0} \left[\frac{Nu_{\beta=0}}{Nu_{\beta=90}} \right]^{\frac{\beta}{\beta_{cr}}} (\sin \beta_{cr})^{\frac{\beta}{4\beta_{cr}}} \tag{1}$$

The Nusselt number for the horizontal, $\beta = 0$, and vertical, $\beta = 90$, positions of SAH are:

$$Nu_{\beta=0} = 1 + 1.44 \left[1 - \frac{1708}{Ra} \right]^+ + \left[\frac{Ra^{\frac{1}{3}}}{18} - 1 \right]^+ \tag{2}$$

$$Nu_{\beta=90} = 0.22 \left(\frac{Pr \cdot Ra}{0.2 + Pr} \right)^{0.28} \left(\frac{H}{L} \right)^{0.25} \tag{3}$$

While the Nusselt number for inclined solar air heater for $0 < \beta < \beta_{cr}$ and $L/H \geq 12$ is:

$$Nu_{\beta} = 1 + 1.44 \left[1 - \frac{1708}{Ra \cos \beta} \right]^+ \left(1 - \frac{1708(\sin(1.8\beta))^{1.6}}{Ra \cos \beta} \right) + \left[\frac{(Ra \cos \beta)^{\frac{1}{3}}}{18} - 1 \right]^+ \tag{4}$$

where,

β : tilt angle of the collector

β_{cr} : critical angle

Nu_{β} : Nusselt number at tilt angle

Ra : Rayleigh number of flowing air, which calculated by:

$$Ra = \frac{g \cdot \bar{\beta} \cdot \Delta T \cdot H^3}{\nu^2} Pr \tag{5}$$

where,

g : The gravitational constant, m/s^2

H : The characteristic length (height of the solar collector), m

ν : Kinematic viscosity, m^2/s

ΔT : Temperature difference between the plate and the cover, K

$\bar{\beta}$: Coefficient of thermal expansion, K^{-1} ($\bar{\beta} = \frac{1}{T_M}$, and $T_M = \frac{T_P + T_g}{2}$)

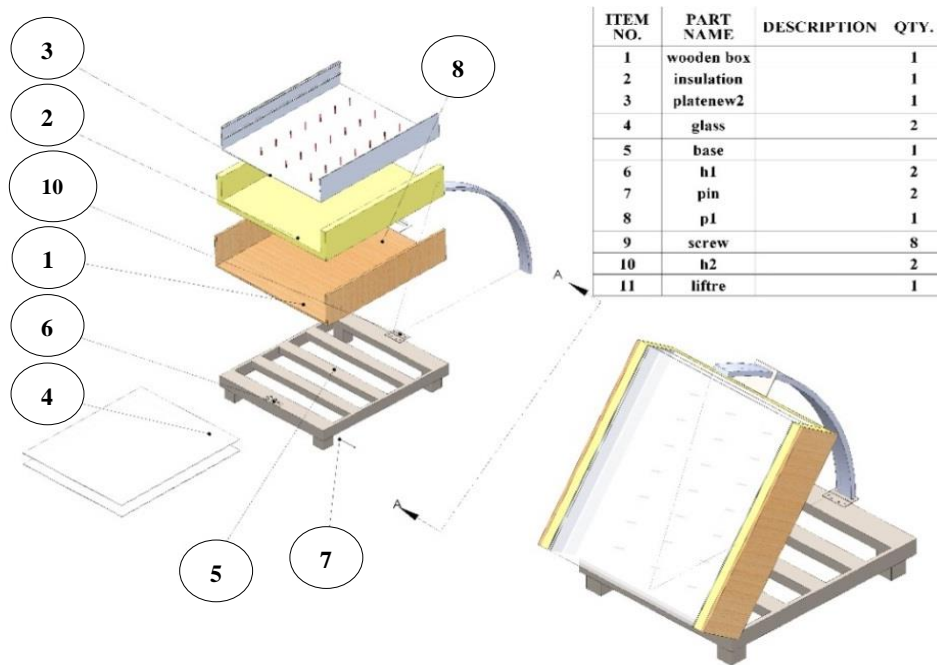
Pr : Prandtl number

For a specific heat transfer coefficient in free convection mode, h ($W/m^2 \text{ } ^\circ C$) of air at certain tilt angle and thermal conductivity, k ($W/m \text{ } ^\circ C$); the hydraulic diameter is determined by Eq. (6), then the width of the collector, W , is obtained from Eq. (7).

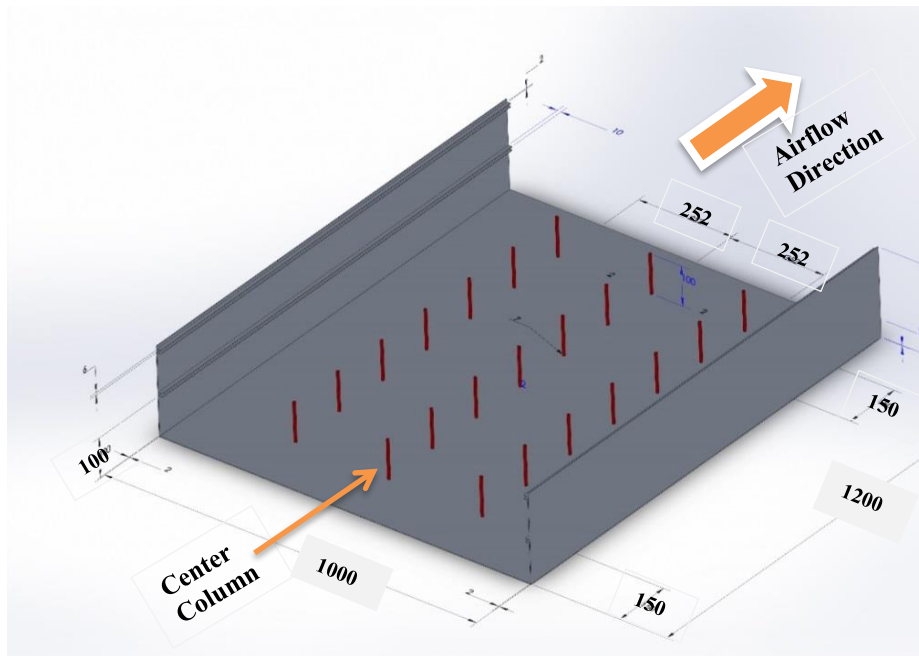
$$Nu_{\beta} = \frac{h D_h}{k} \tag{6}$$

$$D_h = \frac{4HW}{2(H + W)} \tag{7}$$

To determine the experimental model dimensions, predicted data obtained by Bahrehmand and Ameri [12] are adapted. For an aspect ratio of 6, the collector length is $L = 1.2$ m, and the height is $H = 0.2$ m. The calculations run gave the Nusselt number and the Rayleigh number at a 45° tilt angle of 18.376 and 61389870, respectively. Then, the hydraulic diameter of $D_h = 0.334$ m and the collector width of $W \approx 1$ m is obtained. Therefore, the dimensions of the designed model are $L = 1.2$ m, $W = 1$ m, and $H = 0.2$ m, which transferred to the experimental model fabrication. The components of the experimental model with obtained design dimensions are drawn by the SOLIDWORKS software. The positions of thermocouples, the glass covers, thermal insulation material, and the wooden enclosure are specified with all dimensions, as shown in Figure 2.



(a) The solar air heater components



(b) Dimensions of the absorber-plate, covers height, and thermocouples positions in mm

Figure 2. SOLIDWORKS design of the solar air heater

Experimental Setup

The designed dimensions of the solar air heater of 120 cm, 100 cm, and 20 cm in length, width, and height respectively are utilized in the experimental model building. The solar air heater is relying on the absorber-plate component which

collects solar irradiance. In the present study, the absorber plate is made of galvanized steel (thermal conductivity of 60 W/m.K) black coating with a 2 mm thickness. To measure the air temperature distribution along the solar collector, twenty-one vertical rods in three columns distributed by seven rods in each column made on the absorber, as shown in Figure 2-b. The reason for using vertical rods is date back to install thermocouples type-K vertically on the rods. Two types of vertical rods are used based on the transparent cover height, the first level is 20 cm in height and the second is 10 cm. The glass-wool material with thermal conductivity of 0.038 W/m.K used to decrease thermal losses from back of the collector and its sides to the environment. The thickness of the installed insulation material is 2.5 cm on both sides and 5 cm on the backside of the absorber. Then, the absorber and the insulation layers have immersed within a wooden enclosure. Glass covers with 0.9 transmittances and 6 mm thickness are used at the top of the heater channel. Two glass covers utilized for the height 10 cm and 20 cm above the absorber-plate. The steel structure is constructed to test the solar air heater at different inclination angles. The solar air heater has mounted on the movable frame with two curved slide columns to compose four angles; 30°, 45°, 60°, and 75°. Figure 3 shows the full structure of the experimental model of the SAH with a moving frame and thermocouples-thermometers.

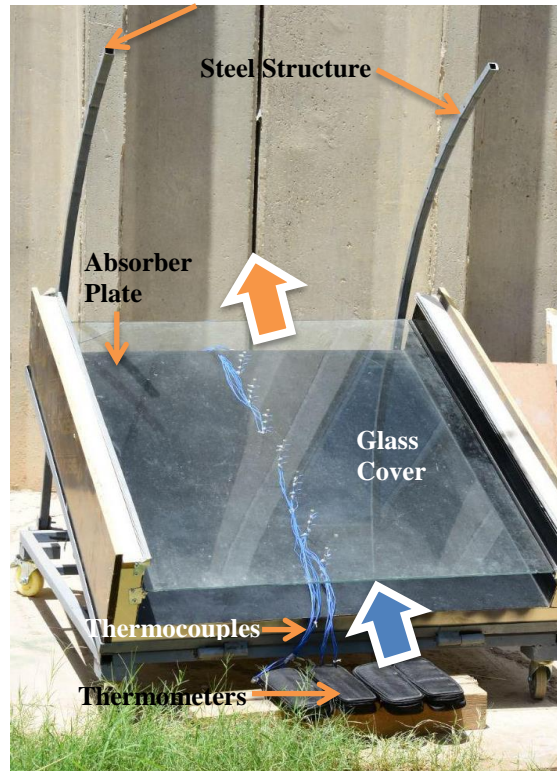


Figure 3. Photograph of experimental model of the SAH (height 10 cm)

Experimental Measurements and Sets

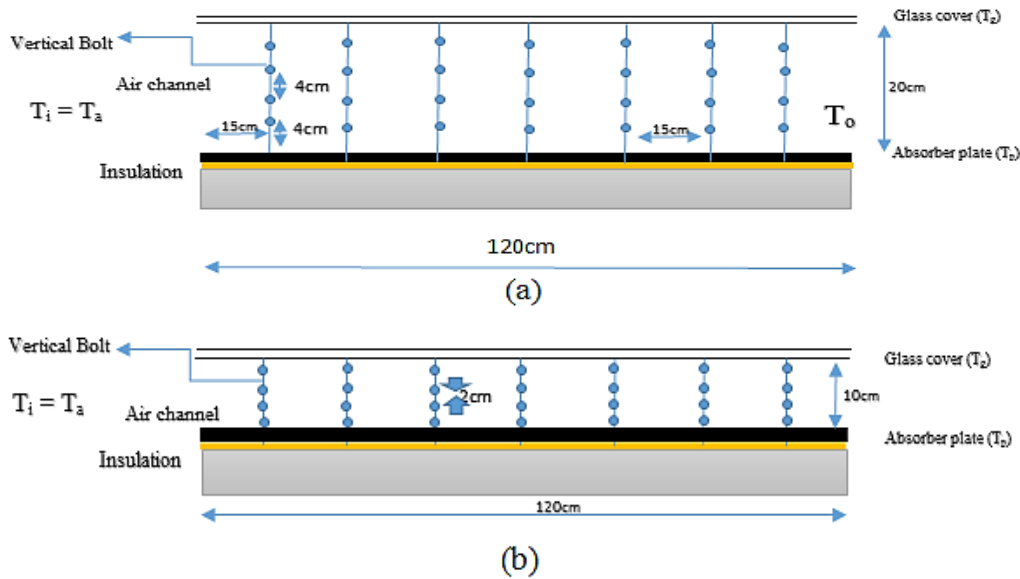
Thermocouples type-K installed on seven rods in a distribution manner include four thermocouples on each one, so twenty-eight thermocouples have used in measuring air temperature along the collector channel for one column. The main measurements were carried out at the center column shown in Figure 2-b, then for the left side column, which is identical to the right side. Every four thermocouples are connected to one microprocessor thermometer to measuring the temperatures of hot airflow, thus seven thermometers were used. The thermocouples are distributed equally in the vertical distance on the used rods for both heights (10 cm, 20 cm), as shown in Figure 4. In cases of 10 cm and 20 cm in height, the distance between thermocouples is 2 cm and 4 cm, respectively. As well, between thermocouple and absorber plate and between thermocouple and glass cover.

The temperatures of the absorber and the glass are measured by using an infrared thermometer unit by taking several readings at different positions. While the speed of airflow within the collector is measured by using an anemometer ranged between 0.2 to 5.0 m/s. The solar irradiance incident on the collector is measured by using the solar meter ranged between zero to 1200 W/m².

The solar air heater has directed to the south orientation in all experimental tests at Baghdad location, where the measurements are carried out from May to October 2018 during the period between 7 am to 3 pm. Test sets studied in the present research are based on the collector height, inclination angles, and with/without airflow passing through the heater channel. Table 2 describes the experimental cases.

Table 2. Experimental cases

Case No.	Collector height	Airflow within the collector	Collector ends	Main measurement	Collector tilt angle
1	20 cm	Yes	Opened	Temperature distribution along the collector	30°, 45°, 60°, 75°
2	10 cm	Yes	Opened		
3	10 cm	No	Closed		
4	10 cm & 20 cm	Yes	Opened	Outlet air temperature	


Figure 4. Positions of the measuring points along the SAH (a) 20 cm height, (b) 10 cm height

Experimental Test Procedure

Before each test, it is a substantial to ensure that the solar air collector is facing the south orientation and checking the position of thermocouples proportionally to the case that tested. Subsequently, the measurements are carried out outside the mechanical engineering laboratory at AL-Nahrain University, Baghdad (latitude of 33.3°N and longitude of 44.4°E), in the period between May to October 2018. The solar air heater has tested for the cases described in table 2 as below:

1. Adjusting the experimental rig for the cover height of 20 cm, inclination angle of 30°, and thermocouples at the center column position of the solar heater.
2. The measurements of twenty-eight readings of air temperatures in seven thermometers, the solar irradiance, temperatures of the absorber plate and glass cover, inlet/outlet air temperature and velocity to/from the solar heater are recorded at 7 am.
3. The procedure in point 2 replicated for hours from 8 am to 3 pm. The heated air flow through the heater channel has recorded at the steady state conditions at the end of each hour.
4. The procedure in points 1, 2, and 3 replicated for the tilt angles of 45°, 60°, 70° (case 1).
5. The procedures in points 1, 2, 3, and 4 replicated for the heater channel height of 10 cm (case 2).

This procedure of multi tilt angles presented in points 1-5 are repeated for the measurements of thermocouples at the position of the left column in the solar heater with heights 10 cm and 20 cm. For the case 3, the procedure elaborated in points 1-5 is repeated for all tilt angles and height 10 cm but without airflow through the solar air heater (closed ends).

The last test case 4 is implemented to measure inlet/outlet air temperature to/from the SAH after the solar irradiance on the absorber plate is interrupted. Then the time needed to reach air temperature equivalence between outlet and inlet is estimated. This time called the time constant of the solar collector which represents the heat capacity saved within the SAH.

Data Analysis

Several parameters are involving heating air in the solar collector. The solar incidence, irradiance absorbed by the plate, losses from the collector, heat gain, and thermal efficiency of the solar air collector were analyzed. To analyze the present solar collector parameters, the following assumptions considered: airflow within the collector is homogeneous, and there is one-dimensional natural convection flow along the collector.

The solar air collector is facing south orientation during the test time. Hence, the solar irradiance falls on the collector surface by different angles; declination angle (δ), surface azimuth angle (γ), hour angle (ω), incidence angle (θ), zenith angle (θ_z), solar altitude angle (ψ), and solar azimuth angle (γ_s) have calculated [1].

The total irradiance (I_T) incident on the absorber-plate consists of the beam irradiance (I_B) that has passed through the atmosphere without being appreciable scattered and the diffuse irradiance (I_D) that reaches the surface after been significantly scattered by the atmosphere [22]. Therefore,

$$I_T = I_B + I_D \tag{8}$$

The beam and diffuse irradiance can be calculated by;

$$I_B = I_{BN} \cos \theta \tag{9}$$

$$I_D = I_{BN} C \left(\frac{1 + \cos \beta}{2} \right) \tag{10}$$

I_{BN} is the normal beam irradiance incident perpendicular to a surface. It is estimated using the ASHRAE clear sky model [23] given by the following equation:

$$I_{BN} = \frac{A}{B / e^{\sin \psi}} \tag{11}$$

where,

$$A = 1158 \left[1 + 0.066 \cos \left(\frac{360N}{365} \right) \right]$$

$$B = 0.175 \left[1 - 0.2 \cos (0.93N) \right] \times 0.0045 \left[1 - \cos (1.86N) \right]$$

$$C = 0.0965 \left[1 - 0.42 \cos \left(\frac{360 \times N}{370} \right) \right] - 0.0075 \left[1 - \cos (1.95N) \right]$$

N: Number of the day in a year

Nevertheless, a part of the total irradiance has throwback to the sky, another part has absorbed by the glass cover and the remains has transmitted via the cover and arrives the absorber. The absorbed energy by the plate, S , is [22]:

$$S = (\tau \alpha)_{avg} I_T \tag{12}$$

where,

$(\tau \alpha)_{avg}$: Average transmittance-absorptance of the collector cover

The heat losses from the solar collector can be divided into two components; top heat losses (U_t), back heat losses (U_b), where the sum of these losses called the overall loss coefficient (U_L) [1]:

$$U_L = U_t + U_b \tag{13}$$

Back loss coefficient, in the unit of (W/m².K), is the losses through the insulation, which calculates from:

$$U_b = \frac{K}{x} \tag{14}$$

where,

K : Thermal conductivity for the glass wool (0.038 W/m.K)

x : Thickness of insulation, m

Top loss coefficient, in the unit of (W/m².K), is the losses occur above the absorber plate and given by:

$$U_t = \frac{\frac{1}{N_g}}{\frac{C}{T_p} \left[\frac{T_p - T_a}{N_g + f} \right]^{0.33} + \frac{1}{h_w}} + \frac{\sigma(T_p^2 + T_a^2)(T_p + T_a)}{\frac{1}{\epsilon_p + 0.05N_g(1 - \epsilon_p)} + \frac{2N_g + f - 1}{\epsilon_g} - N_g} \tag{15}$$

where,

$$f = (1 - 0.04h_w + 0.0005h_w^2) (1 + 0.091 N_g)$$

h_w : the convection heat transfer coefficient of the wind, which determined by [$h_w = 2.8 + 3\sqrt{V}$]

V : wind velocity, m/s

- $C = 365.9(1 - 0.00883\beta + 0.0001298\beta^2)$
- σ : Steven Boltzmann constant ($5.67 \times 10^{-8} \text{ W/m}^2 \cdot \text{K}^4$)
- T_p : Mean plate temperature, K
- T_a : Ambient air temperature, K
- N_g : Number of glass cover
- ϵ_p : Emissivity of plate (0.95)
- ϵ_g : Emissivity of glass (0.88)

Under steady-state conditions of heating air in the collector, the useful heat gain, Q_u , obtained from the solar collector is the diversity between the absorbed solar irradiance and the thermal losses. Useful heat gain can be determined as below [1]:

$$Q_u = A_c [S - U_L(T_p - T_a)] \tag{16}$$

where A_c is the surface area of the collector.

The solar air collector performance evaluated by the collector efficiency, η , which defined as the ratio of the useful heat gain (Q_u) to the incidence solar irradiance on a specific time, the efficiency can be calculated as [1]:

$$\eta = \frac{Q_u}{A_c I_T} \tag{17}$$

Natural convection caused by changing the air density in the streamlines due to temperatures difference and the buoyancy force. Therefore, a dimensionless quantity of the Grashoff number, Gr , was adopted, which represents the buoyancy force to the viscous force. A significant dimensionless quantity that evaluates the natural convection flow is the Rayleigh number, Ra , which is given by Eq. (5).

Nusselt as a dimensionless number indicates the amount of heat transferred by conduction that measured under the same conditions as the amount of convection heat, but with the assumption of stagnant fluid. The Nusselt number estimated by Eq. (1) was utilized to calculate the coefficient of natural convection heat transfer, h .

The experimental measurements for the case of the tilt angle of 45° , the collector height of 10 cm, the test position is center, and the date of the test is 7th June 2018 shown in Table 3. These data were analyzed and the outcomes shown in Table 4.

Table 3. Experimental measurements dated 7 June 2018

Time (hr)	Solar Irradiance (W/m ²)	Mean Plate Temp. (°C)	Mean Cover Temp. (°C)	Ambient Air Temp. (°C)	Collector Inlet Air Velocity (m/s)	Collector Outlet Air Temp. (°C)	Collector Outlet Air Velocity (m/s)
7:00 am	181	32	29	28	0.01	29.9	0.1
8:00 am	264	40	33	30	0.01	33.5	0.4
9:00 am	568	62	43	37.5	0.46	41.3	0.9
10:00 am	649	75	44	41.9	0.32	48	0.67
11:00 am	728	81	47	47.8	0.4	52.9	0.41
12:00 pm	707	88	49.5	46	0.3	50.2	0.6
1:00 pm	692	89	50	46	0.2	54	0.49
2:00 pm	491	77	48	44	0.59	50	0.48
3:00 pm	462	63.8	45	42	0.16	48	0.53

Table 4. Analytical outcomes

Time (hr)	Absorbed Irradiance, S (W/m ²)	Useful Energy, Q _u (W)	Efficiency, η (%)	Rayleigh Number	Nusselt Number, Nu _β	Convection Coefficient, h (W/m ² .K)
7:00 am	38.438	53.892	17.722	6440107	12.266	1.783
8:00 am	144.554	217.069	48.942	13725504	15.268	2.255
9:00 am	394.325	594.078	62.256	29650861	19.179	2.951
10:00 am	479.858	707.741	64.911	44020221	21.606	3.383
11:00 am	547.378	815.081	66.643	45510878	21.825	3.455
12:00 pm	533.725	762.793	64.221	48482017	22.248	3.562
1:00 pm	520.311	737.530	63.440	48646210	22.271	3.572
2:00 pm	363.036	509.296	61.741	39584658	20.922	3.299
3:00 pm	320.736	476.296	61.365	28587747	18.971	2.933

Uncertainty in Measurements

The precision of obtaining experimental results relies on two factors, the accuracy of measurements and the design details of the test rig. The deviations in measurements came from; the observation, alignment of fixing thermocouples on the rods, and errors in the measuring instruments.

There is no doubt, the errors in the estimated results referred essentially to the errors in the measured quantities. The measured parameters in the present experiments are ambient temperature, solar irradiance, temperature and velocity of inlet/outlet collector, the surface temperature of the absorber and transparent cover, and temperature of the airflow in the solar heater.

The procedure of Kline and McClintock (Holman, 2001) is used to calculate the error. Hence, the uncertainty, *W*, for the variable *R* in the non-dimensional or fractional form is [24]:

$$\frac{W_R}{R} = \left[\left(\frac{\partial R}{\partial v_1} \cdot \frac{w_1}{R} \right)^2 + \left(\frac{\partial R}{\partial v_2} \cdot \frac{w_2}{R} \right)^2 + \dots + \left(\frac{\partial R}{\partial v_n} \cdot \frac{w_n}{R} \right)^2 \right]^{1/2} \tag{18}$$

The efficiency of the solar air heater calculated by Eq. (16) is a function of several variables, where each subjected to uncertainty. The useful heat gained to the collector has transferred to the air flowing in the collector. Thence, the solar air heater efficiency can be expressed as:

$$\eta = \frac{\dot{m} C_p \Delta T}{A_c I_T} \tag{19}$$

where,

- Δ*T*: Temperature difference between outlet and inlet of the collector (*T_o* – *T_i*), K
- m*: Mass flow rate of air(ρ*Va*), kg/s
- V*: Air velocity, m/s
- a*: Cross sectional area of the collector, m²

The variables associated with the efficiency of the solar collector are; air velocity, temperature difference, and total solar irradiance. Hence,

$$\eta = f(V, \Delta T, I_T) \tag{20}$$

The experimental errors that occur in the applied variables are associated with accuracy shown in Table 3, which adopted from measuring instrument catalogs.

Table 5. Measuring instruments accuracy

Independent Variables	Accuracy of readings
Air velocity	± 5% m/s
Air temperature	± 1% °C
Incident irradiance	± 3% W/m ²

The fractional uncertainty of the estimated thermal efficiency based on Eq. (20) for air velocity(∂η/∂*V*), air temperature difference(∂η/∂Δ*T*), and total solar irradiance (∂η/∂*I_T*) is shown in Eq. (21).

$$\frac{W_{\eta}}{\eta} = \left[\left(\frac{\partial \eta}{\partial V} \cdot \frac{W_V}{\eta} \right)^2 + \left(\frac{\partial \eta}{\partial I_T} \cdot \frac{W_{I_T}}{\eta} \right)^2 + \left(\frac{\partial \eta}{\partial \Delta T} \cdot \frac{W_{\Delta T}}{\eta} \right)^2 \right]^{1/2} \quad (21)$$

For an incident solar irradiance of 707 W/m², air velocity of 0.6 m/s, and air temperature difference of 4.2°C, the thermal efficiency of the solar air collector is 64.22%. Thence, the calculated uncertainty of the thermal efficiency for these measured parameters is 0.0344, which demonstrates acceptable value and so as for the other cases.

RESULTS AND DISCUSSIONS

The obtained results from experimental tests and data analysis have presented in the next section.

Experimental Results

Air temperature distribution along the collector

The temperature of the absorber-plate is rising due to solar irradiance receiving. Hence the temperature of the air flowing within the collector is increasing. The airflow temperature distribution along the solar collector for different tilt angles and the heights of 10 cm and 20 cm have compared and tested at 1 pm and 12 pm respectively, as shown in Figure 5. The results show the behavior of airflow temperature gradient within the heater channel, where the temperature increases when distance along the absorber-plate increase due to heat transfer, except the decreasing of temperature at distance 120 cm because of ambient effect. The tilt angles of 30°, 45°, 60°, and 75° have a significant effect on the temperature distribution through the collector especially for the height 10 cm, where the highest air temperatures occur at an inclination angle of 30°. The Figure shows, clearly, the temperature values for all inclination angles at the height of 10 cm greater than those at the height of 20 cm. The reason dates back to the lesser height of the collector which keeps the hot air produced by the convection and radiation heat within the solar air collector at high temperatures.

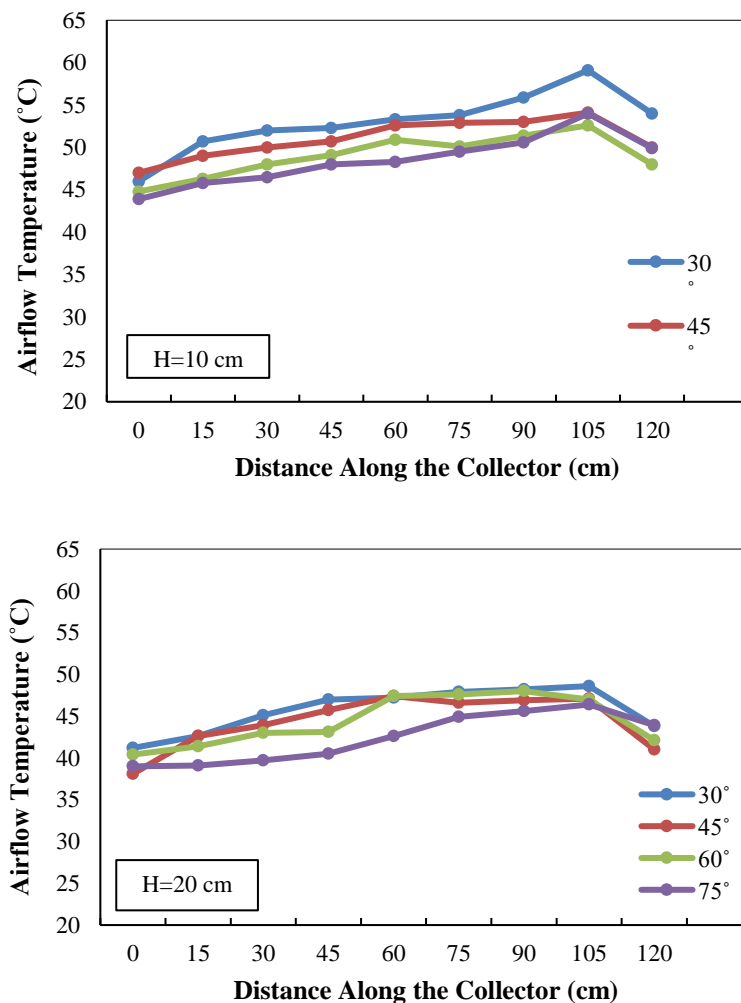


Figure 5. Airflow temperature distribution along the solar air collector for heights 10 cm, 20 cm, and different tilt angles (17/5/2018)

Comparison of temperatures distribution

To compare airflow temperature distribution along the collector between the positions of the center column and side column, Figure 6 shows the distribution comparison of air temperatures between the center and the left side position at 1 PM, tilt angle of 45°, and the height of 10 cm. The results show that the temperatures of the center position are higher than the side position due to the buoyancy effect of hot air when passing through the collector, where it concentrates at the collector center and decreases at the sides. It is found that the results of average airflow temperatures for the center position are higher than the side position by 6%.

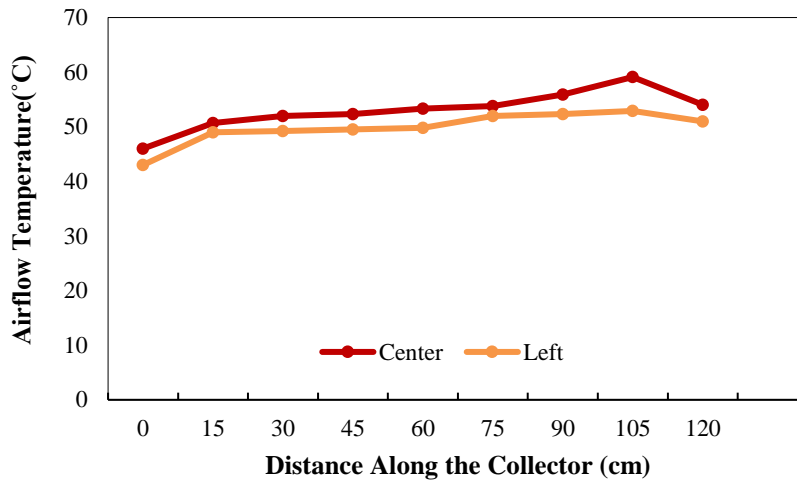


Figure 6. Temperature distribution along the solar air collector for the center and left position tilt angle of 45°, and H=10 cm (17/5/2018)

Figure 7 shows the comparison of temperature distribution along the solar air heater between the height of 10 cm and 20 cm at 1 PM and the tilt angle of 45°. The results show that air temperatures for the height of 10 cm are higher than that for the height of 20 cm due to producing high temperatures within the lesser height of the solar air collector, which converts from the solar irradiance absorbed by the plate. It is found that the results of average airflow temperatures for the height of 10 cm are higher than that for the height of 20 cm by 23%.

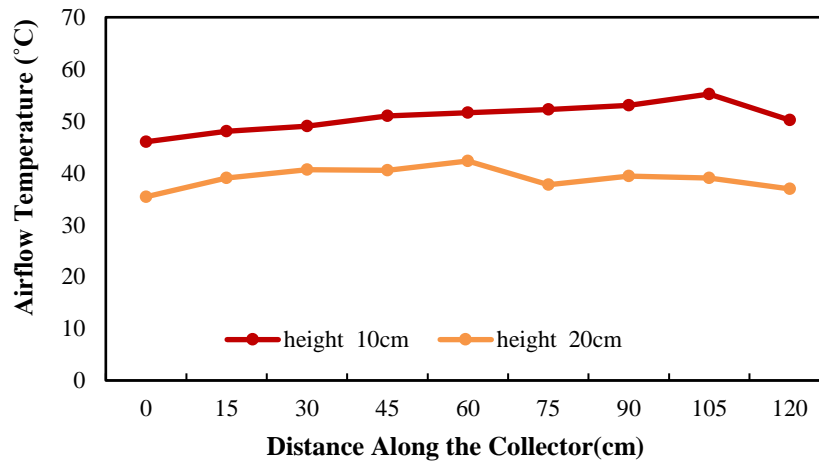


Figure 7. Temperature distribution along the solar air collector for the height of 10 cm and 20 cm and tilt angle of 45° (17/5/2018)

Solar collector without airflow (closed ends)

The temperature distributions through the solar air heater for the cases with/without airflow, different tilt angles, and height of 10 cm are shown in Figure 8. The Figure shows the values of air temperatures along the solar collector according to thermocouples positions shown in Figure 4. The results reveal air temperatures for the case without flow (closed ends) are greater than that for the case with the flow (open ends). These results are decreasing when the tilt angles increase from

30° to 75°. The percentage of air temperature rise between closed and open ends cases ranges from 15.4% to 43% for the tilt angle of 30°, and from 0% to 36.7% for the tilt angle of 75°. It is found that in the absence of airflow in the solar heater, the obtained air temperatures up to 103°C for the tilt angle of 30°, which can be used for drying the crops of plants.

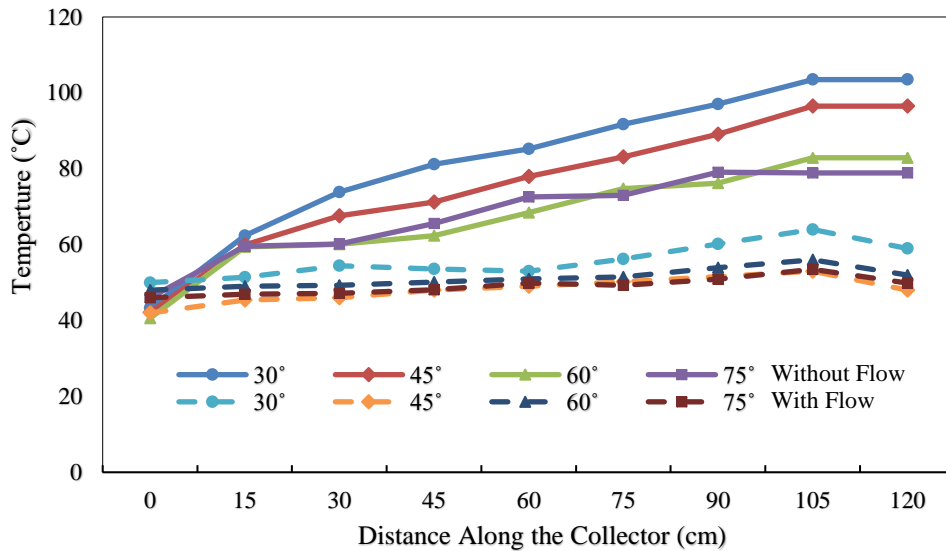


Figure 8. Temperature distribution along the solar air collector for the cases with / without airflow, different tilt angles, and $H = 10$ cm (24/9/2018)

2D Air temperatures distribution

The temperature stratification of hot air through natural convection flow in the solar collector is shown in Figures 9 and 10. The Figures show air temperatures contours vary in two dimensions, along the solar collector of 120 cm in length and the heights of 10 cm and 20 cm. The blue color shined in these Figures reveals and refers to the ambient air entering the heater channel and moves decreasingly along the collector due to air buoyancy. The heat transferred from the heated absorber-plate at the collector's bottom to air flowing in the heater channel. Therefore, air temperatures are more stratified near the collector's bottom and diminishingly toward the collector cover.

Figure 9 shows air temperatures contours within the solar air heater for different tilt angles and height of 10 cm. Temperatures contours graded from high temperature at absorber-plate to the ambient temperature layer bounded by blue color line at the top. Thermal behavior shows an increase in the boundary layer in the hot air flow via the collector channel when the distance along the collector increases toward the outlet. Also, when the tilt angles increase from 30° to 75°, Figure 9 shows increasing the thickness of the thermal layer growing on the absorber-plate due to increasing the buoyancy force induce the hot air in the natural convection flow. The temperature stratification is clearly revealed in the solar air heater with a height of 10 cm.

Figure 10 shows air temperatures contours within the solar air heater for different tilt angles and height of 20 cm. When the height of the collector doubled, Figure 10 shows lesser stratification in the top half of the collector in comparison with Figure 9. Ambient air blocks pulled through the collector channel are revealed in Figure 10 due to increasing the collector height. When the tilt angles increase from 30° to 75°, Figure 10 shows increasing the thickness of non-regular thermal layers at the top half and along the collector with air blocks movement, the reason dates back to the very low speed for the buoyant hot air. Also, the temperature of air blocks and thermal layers close to the transparent cover is increasing at a high tilt angle.

In conclusion, regular stratification of hot air in natural convection flow has achieved when the collector height decreases. The thermal boundary layer increases in the natural convection flow when increasing the distance along the collector plate.

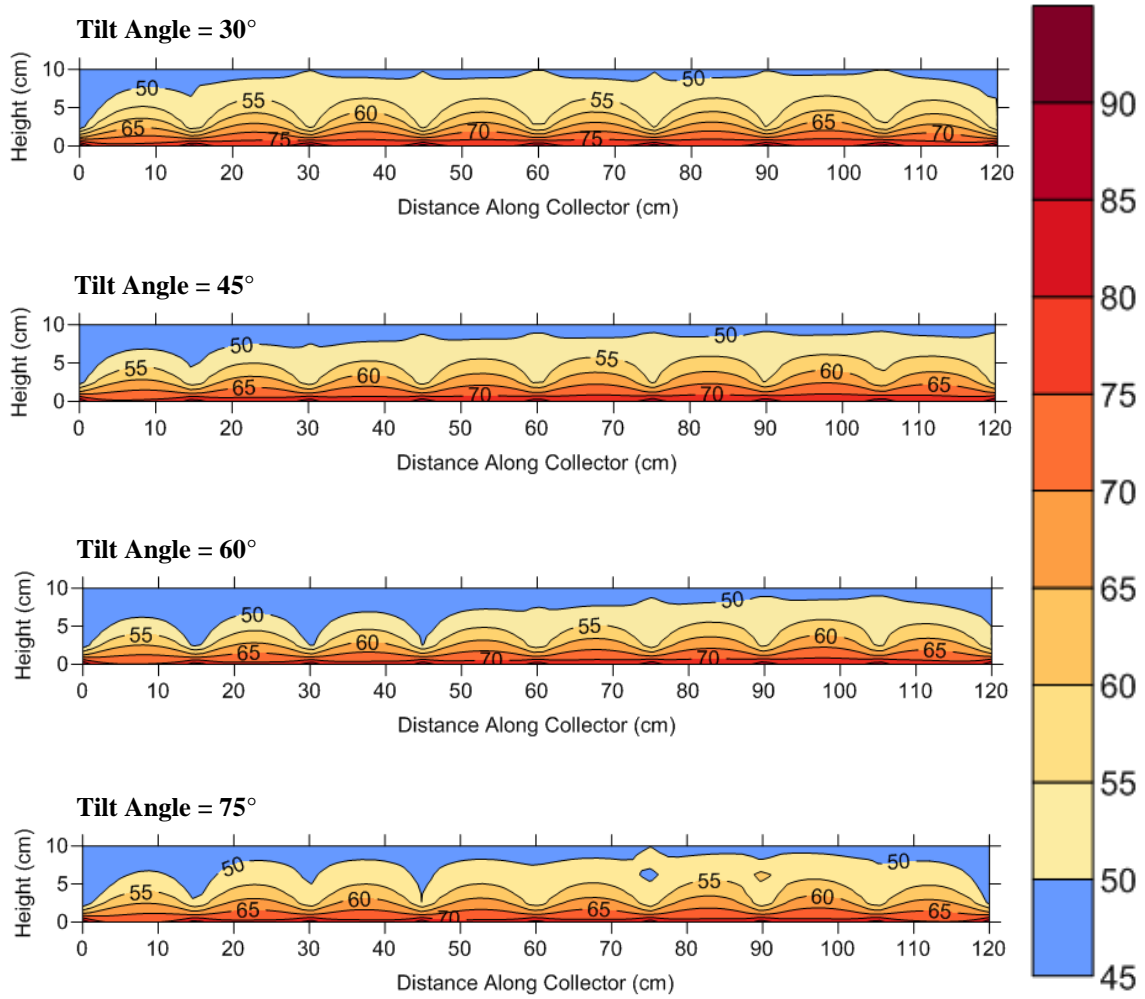


Figure 9. 2D contour results of temperature distribution in 10 cm height solar air collector for different tilt angles, 12 pm (6–9/6/2018)

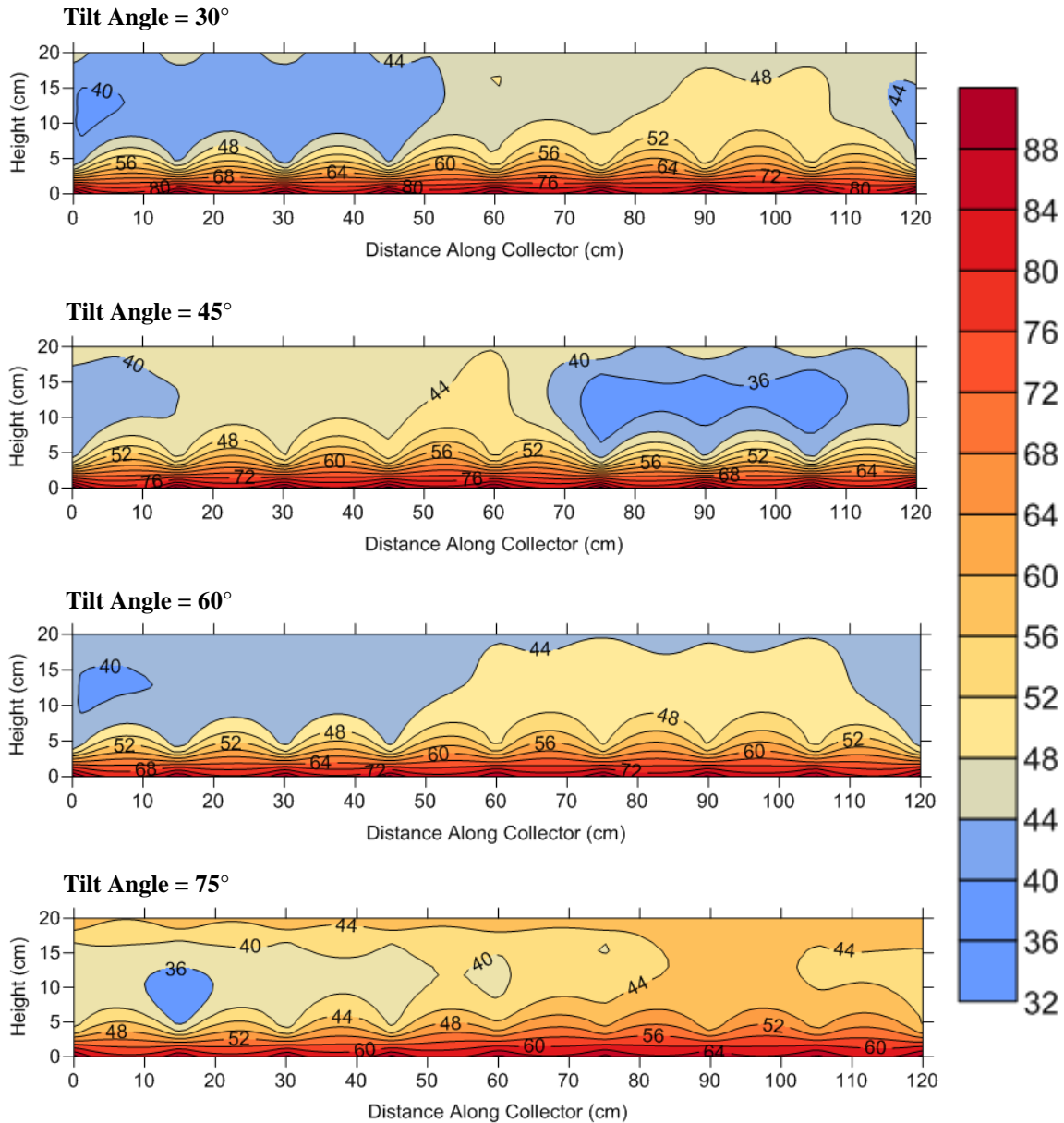


Figure 10. 2D contour results of temperature distribution in 20 cm height solar air collector for different tilt angles, 12 pm (22–28/5/2018)

Remarkable measurement of heat capacity

The other side of collector testing is the definition of the heat capacity of the solar collector in terms of the time constant. The time constant is the time needed for air leaving the collector to change through $(1 - 1/e) = (0.632)$ of the whole change from the initial point of the solar interruption to the steady-state of inlet air temperature, which gives the outlet air temperature as a function of the time change. The time constant of the solar collector, t , is determined by [1]:

$$\frac{T_{o,t} - T_i}{T_{o,init} - T_i} = \frac{1}{e} = 0.368 \tag{22}$$

where $T_{o,t}$ is the outlet temperature at time t , $T_{o,init}$ is the outlet temperature when the solar irradiance is interrupted, and T_i is the inlet or ambient temperature. The solar air collector is tested at a steady-state condition of receiving irradiance, and then the outlet air temperature from the solar collector is measured and so as the ambient air temperature. Subsequently, the time for the temperature to drop to 0.368 of the total possible drop is determined, that is, for B/A shown in Figure 11 to reach the value 0.368.

Figure 11 shows a sample of the measurements of the outlet temperature versus time for the flat-plate solar air heater ($\beta=30^\circ$, $H=10$ cm, and $T_{amb}=34^\circ\text{C}$) when the received solar irradiance is interrupted. The Figure shows decreasing the outlet air temperature to the ambient air temperature when the time increases, so the time constant of 7.5 min is estimated.

The test procedure for the solar air heater repeated for all inclination angles and the collector heights of 10 cm and 20 cm. The values of time constant are calculated by Eq. (22) and displayed in Table 6. Increasing the values of time constant when the tilt angle decreases illustrate that the heat capacity of the collector rises. Table 6 shows that the time constant for the height of 10 cm higher than that for the height of 20 cm. Also, shows a high reduction in time constant of 46.6 % occurs between height 10 cm and height 20 cm at a tilt angle of 30°. The best heat capacity obtained by the solar air heater is achieved when the tilt angle and the collector height decreases.

Table 6. Time constant for the solar air heater

Angle of Inclination	Height 10 cm			Height 20 cm			Time constant reduction (%)
	T_a (°C)	$T_{o,t}$ (°C)	Time Constant (min)	T_a (°C)	$T_{o,t}$ (°C)	Time Constant (min)	
30°	34.0	44.1	7.5	37.5	43.1	4	46.6
45°	38.1	50.4	4	38.0	42.3	2.4	40
60°	39.6	48.0	2.7	37.5	40.7	1.8	33.3
75°	40.1	47.6	2	37.5	40.3	1.4	30

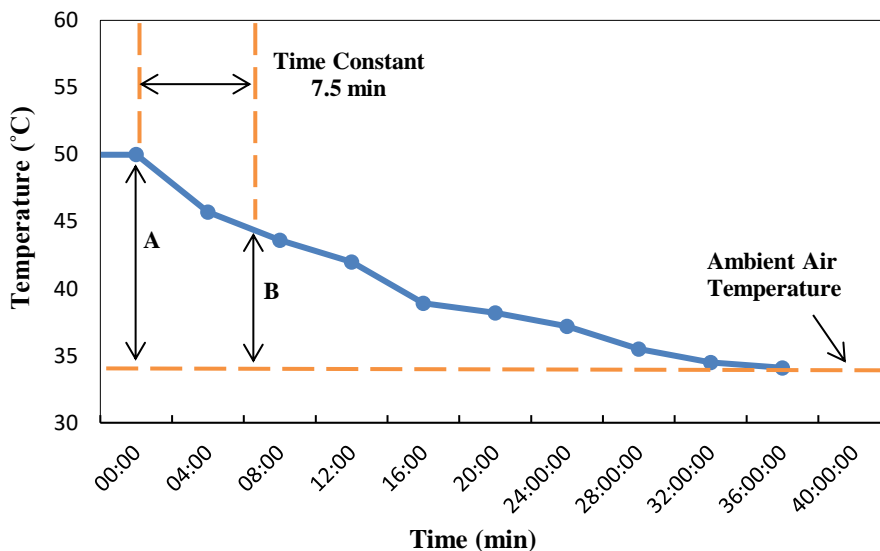


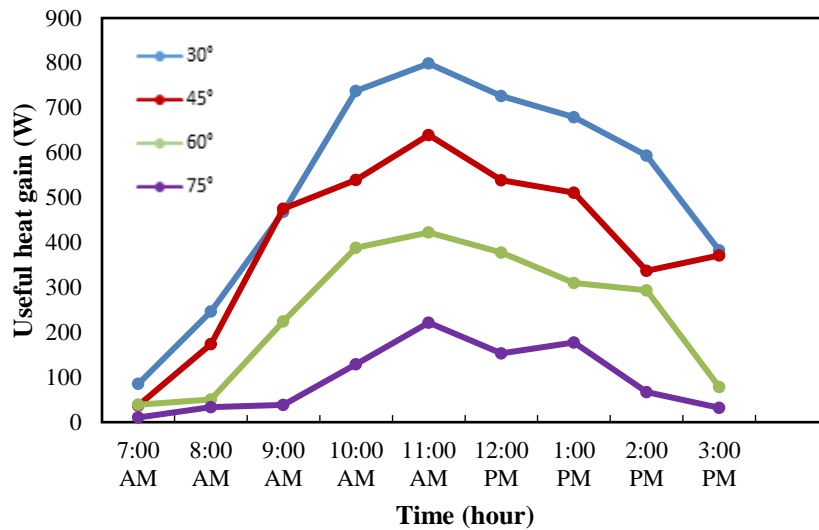
Figure 11. Temperature-Time measurements for the SAH at $\beta=30^\circ$, $H=10$ cm, and $T_{amb.}=34^\circ\text{C}$ when the solar irradiance interrupted at 11 am (30/9/2018)

Analytical Results

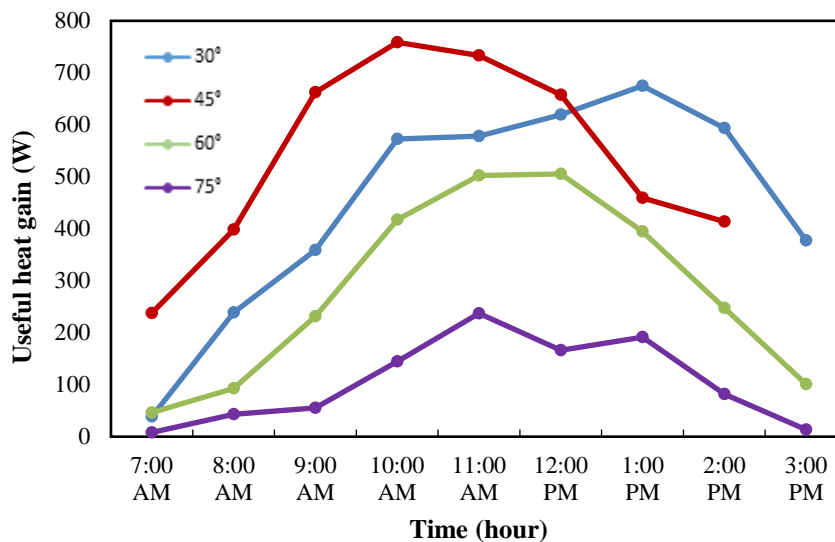
The obtained measurements have been utilized and analyzed to elaborate and describe the thermal behavior of the solar air heater studied in the present work.

Useful heat gain

The useful heat gain, Q_u , as a significant parameter is based on the absorbed solar irradiance, the overall loss coefficient, and the temperature difference between the plate and ambient temperatures. Figure 12 shows the distribution of useful heat gain changing with time, tilt angles, and the collector height of 10 cm and 20 cm. The results reveal increasing the heat gain when the time increases until reaches the highest value at the noon, then drops when the test time arrives at 3 pm. The reason dates back to changing the solar irradiance received by the collector during the test time. The obtained results demonstrate, generally, decreasing in the heat gain by the solar heater when the tilt angle increases. The maximum heat gain of 798.7 W and 758.7 W occurs for the solar air collector at height 10 cm and tilt angle of 30°, and height 20 cm and tilt angle of 45°, respectively. It is found that the maximum heat gain of the solar air heater for the height of 10 cm is higher than for the height of 20 cm.



(a) Height of the collector = 10 cm and measurements period (6–9/6/2018)

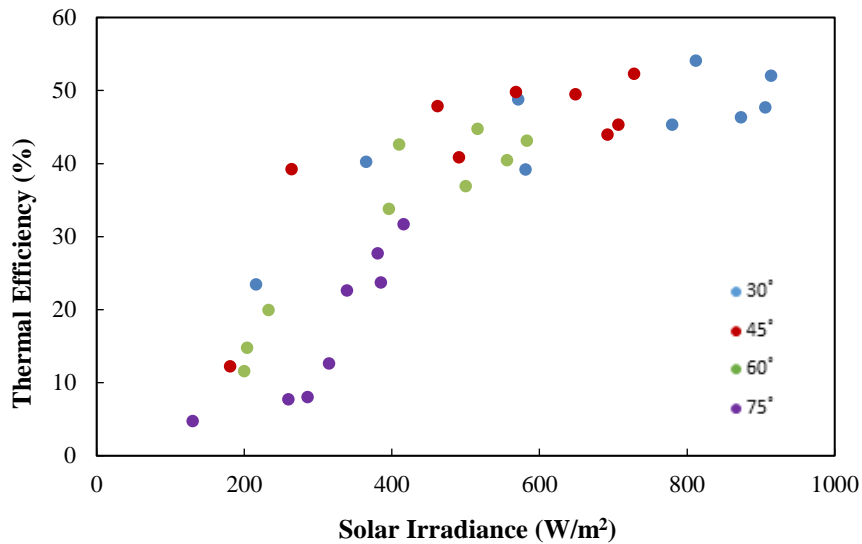


(b) Height of the collector = 20 cm and measurements period (22–28/5/2018)

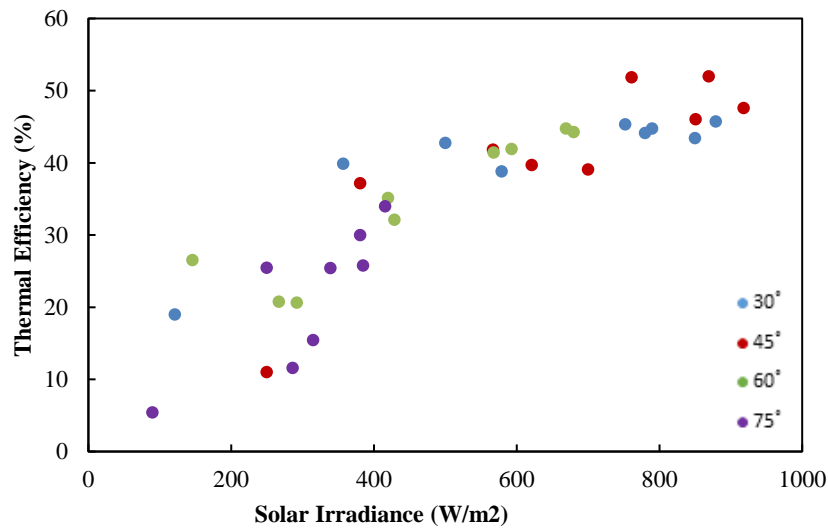
Figure 12. Useful heat gain distribution with time for different tilt angles

Thermal efficiency of the collector

Thermal efficiency shown in Eq. (17) represents the thermal evaluation for the solar air collector and refers to the percentage of the useful energy obtained by the collector to the incident solar irradiance. Figure 13 shows the distribution of thermal efficiency versus the solar irradiance changing during the day for different tilt angles and the collector height of 10 cm and 20 cm. The Figure shows increasing the thermal efficiency when the solar irradiance increases due to increasing the absorbed solar irradiance and then the heat gain. Subsequently, the thermal efficiency decreases when the tilt angle increase based on the magnitude of the absorbed solar irradiance.



(a) Height of the collector = 10 cm and measurements period (6–9/6/2018)

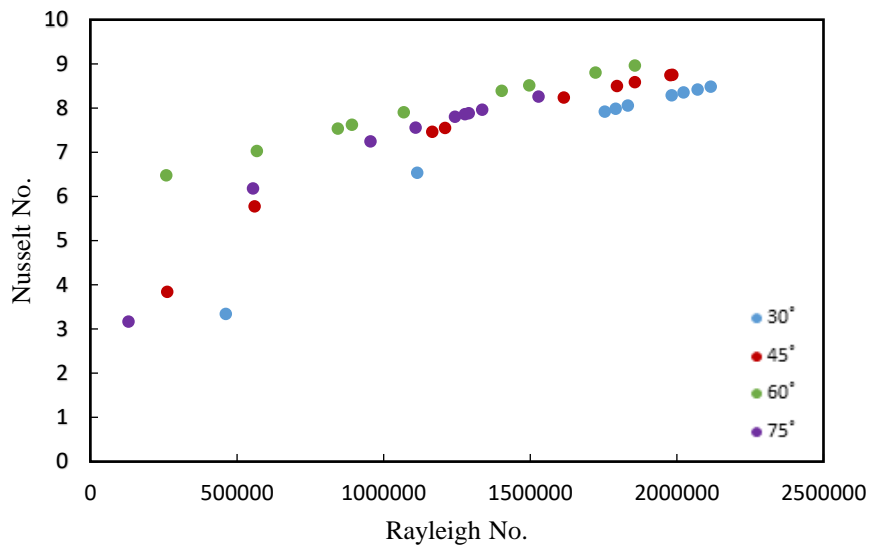


(b) Height of the collector = 20 cm and measurements period (22–28/5/2018)

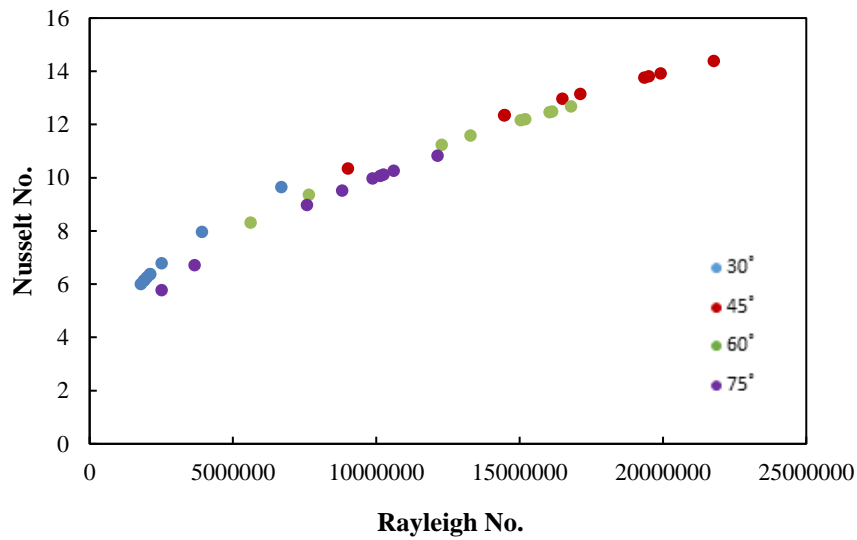
Figure 13. Thermal efficiency distribution versus solar irradiance for different tilt angles

Natural convection flow

To evaluate the natural convection flow within the solar air collector, the dimensionless quantity of Rayleigh number, Ra , and Nusselt number, Nu , are utilized and determined by Eq. (5) and (1), respectively. Figure 14 shows the distribution of $Nu - Ra$ for different tilt angles and the collector height of 10 cm and 20 cm. The Figure shows that the convection heat transfer increases when the buoyant force increase. For the height of 10 cm, the results increase when the tilt angle increases from 30° to 60° then decreases when the tilt angle reaches 75° due to exceed the critical angle described in Table 1. For the height of 20 cm, the results increase when the tilt angle increases from 30° to 45° then decreases when the tilt angles go toward 60° and 75°. The reason dates back to increasing the tilt angle with high gap of the collector, moreover the tilt angle exceeds the critical angle. The estimated results of Rayleigh number are revealing values less than 22×10^6 for the height of 20 cm and values less than 22×10^5 for the height of 10 cm, which reveals buoyant air in the laminar region in the heater channel for the height 20 cm is higher than for the height 10 cm. Therefore, the best convection heat transfer occurs when the collector height decreases, which illustrated the 2D results of the temperature stratification.



(a) Height of the collector = 10 cm and measurements period (6–9/6/2018)



(b) Height of the collector = 20 cm and measurements period (22–28/5/2018)

Figure 14. Distribution of Nusselt number with Rayleigh number for different tilt angles

The collector efficiency

The thermal efficiency of the solar air collector and the temperature difference with incident solar irradiance are utilized to evaluate the solar collector in the present research. Figure 15 shows the efficiency of the flat-plate solar air collector used in the present study. The Figure shows decreasing the thermal efficiency when the temperature difference to the solar irradiance increases. The thermal behavior of the obtained efficiency is in agreement with the previous studies [1]. The thermal behavior of the solar air collector shown in Figure 15 is presented by an experimental relationship as described below.

$$\eta = -2046.8(\Delta T / I_T) + 58.45 \tag{23}$$

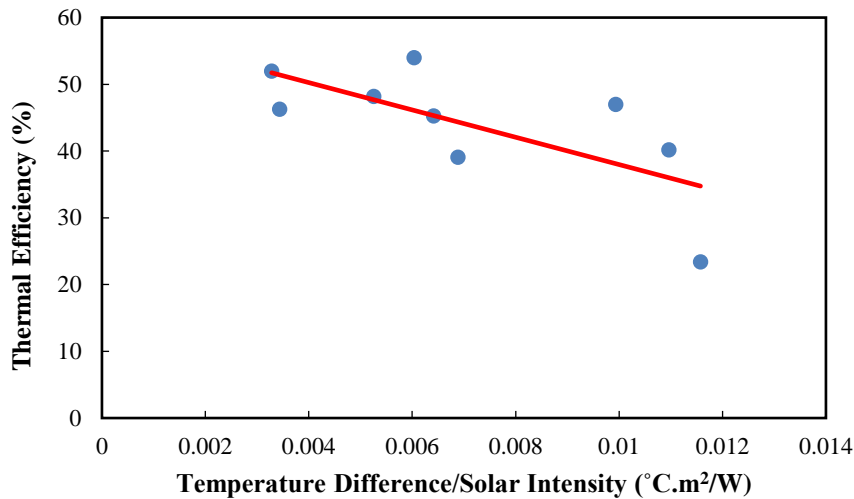


Figure 15. The flat-plate solar air collector efficiency

CONCLUSIONS

The experimental model of the SAH is designed, fabricated, and tested for different heights and tilt angles. The temperature distribution of floated air in an inclined SAH is investigated in 1D and 2D. The obtained 2D air temperature distribution demonstrated regular stratification of hot air in the natural convection flow when the collector height decreases. The results of study show air temperatures increase when distance along the absorber-plate increases due to heat transfer to the buoyant air. It is found that the air temperatures for the height of 10 cm are higher than that for the height of 20 cm by 23%, while the air temperatures for the center position are higher than the side position by 6%. The outcomes of air temperature distribution in 1D and 2D and its position within the SAH can be utilized technically in space heating and passive ventilation for buildings by controlling the positions of air supplies and air exhausts, respectively.

The present investigation finds that the temperature distribution and heat capacity are increasing when the collector height and tilt angles decrease. The heat capacity (time constant) decreases by 46.6 % between height 10 cm and 20 cm for tilt angle of 30°. The convection heat transfer of the floating air increases when the buoyant force of the natural flow increases. When the tilt angle (75°) exceeds the critical angle for the aspect ratio of 12, the results show decreasing in the convection heat transfer due to temperature difference decreases.

ACKNOWLEDGMENTS

The authors would like to acknowledge Al-Nahrain University and mechanical engineering department for logistic and technical support to produce this work. The authors declare that this research did not obtain any particular grant from funding agencies in the public or commercial sectors.

REFERENCES

- [1] J. A. Duffie and W. A. Beckman, "Solar engineering of thermal processes. Hoboken," ed: New Jersey: John Wiley & Sons, Inc, 2013.
- [2] H. H. Al-Kayiem, A. T. Mustafa, and S. I. Gilani, "Solar vortex engine: Experimental modelling and evaluation," *Renewable energy*, vol. 121, pp. 389-399, 2018.
- [3] S. A. Kalogirou, "Solar thermal collectors and applications," *Progress in energy and combustion science*, vol. 30, pp. 231-295, 2004.
- [4] F. P. Incropera, A. S. Lavine, T. L. Bergman, and D. P. DeWitt, *Fundamentals of heat and mass transfer*: Wiley, 2007.
- [5] C. Ya and G. AJ, "Heat and Mass Transfer Fundamentals & Applications," ed: McGraw-Hill, 2015.
- [6] K. Hollands, T. Unny, G. Raithby, and L. Konicek, "Free convective heat transfer across inclined air layers," 1976.
- [7] T. Beikircher, V. Berger, and M. Möckl, "Real-size experiments on reverse natural air convection between inclined parallel plates for new insulation methods in solar flat-plate collectors," *Journal of Solar Energy Engineering*, vol. 139, 2017.
- [8] S. Siddiqa, S. Asghar, and M. A. Hossain, "Natural convection flow over an inclined flat plate with internal heat generation and variable viscosity," *Mathematical and Computer Modelling*, vol. 52, pp. 1739-1751, 2010.

- [9] A. L. Hernández and J. E. Quiñonez, "Experimental validation of an analytical model for performance estimation of natural convection solar air heating collectors," *Renewable Energy*, vol. 117, pp. 202-216, 2018.
- [10] A. Hematian and A. A. Bakhtiari, "Efficiency analysis of an air solar flat plate collector in different convection modes," *International journal of green energy*, vol. 12, pp. 881-887, 2015.
- [11] G. S. Bagga, "Analysis of Flat Plate Solar Air Collector in Different Convection Mode with Induced Turbulence," *International Journal of Engineering Research & Technology*, vol. 5, pp. 488-494, 2016.
- [12] D. Bahrehmand and M. Ameri, "Energy and exergy analysis of different solar air collector systems with natural convection," *Renewable Energy*, vol. 74, pp. 357-368, 2015.
- [13] A. Demou and D. Grigoriadis, "1D model for the energy yield calculation of natural convection solar air collectors," *Renewable Energy*, vol. 119, pp. 649-661, 2018.
- [14] D. Kumar and B. Premachandran, "Effect of atmospheric wind on natural convection based solar air heaters," *International Journal of Thermal Sciences*, vol. 138, pp. 263-275, 2019.
- [15] H. Mzad, K. Bey, and R. Khelif, "Investigative study of the thermal performance of a trial solar air heater," *Case Studies in Thermal Engineering*, vol. 13, p. 100373, 2019.
- [16] A. P. Singh, A. Kumar, and O. Singh, "Designs for high flow natural convection solar air heaters," *Solar Energy*, vol. 193, pp. 724-737, 2019.
- [17] R. P. Garcia, S. del Rio Oliveira, and V. L. Scalon, "Thermal efficiency experimental evaluation of solar flat plate collectors when introducing convective barriers," *Solar Energy*, vol. 182, pp. 278-285, 2019.
- [18] H. Hassan, S. Abo-Elfadl, and M. El-Dosoky, "An experimental investigation of the performance of new design of solar air heater (Tubular)," *Renewable Energy*, vol. 151, pp. 1055-1066, 2020.
- [19] M. Seco-Nicolás, M. A. García, and J. P. Luna-Abad, "Experimental calculation of the mean temperature of flat plate thermal solar collectors," *Results in Engineering*, vol. 5, p. 100095, 2020.
- [20] S. Abo-Elfadl, H. Hassan, and M. El-Dosoky, "Study of the performance of double pass solar air heater of a new designed absorber: An experimental work," *Solar Energy*, vol. 198, pp. 479-489, 2020.
- [21] N. F. Jouybari and T. S. Lundström, "Performance improvement of a solar air heater by covering the absorber plate with a thin porous material," *Energy*, vol. 190, p. 116437, 2020.
- [22] S. A. Kalogirou, *Solar energy engineering: processes and systems*: Academic Press, 2013.
- [23] I. ASHRAE, *ASHRAE handbook: fundamentals*: American Society of Heating, Refrigeration and Air-Conditioning Engineers, 2009.
- [24] J. P. Holman, *Experimental methods for engineers*, 2001.